Journal of Neuropathology and Experimental Neurology

Vol. 58, No. 5
May, 1999
pp. 459–471

Neuronal Death in Amyotrophic Lateral Sclerosis Is Apoptosis: Possible Contribution of a Programmed Cell Death Mechanism

LEE J. MARTIN, PHD

Abstract. The mechanisms for neurodegeneration in amyotrophic lateral sclerosis (ALS) are not understood. We found that motor neuron degeneration in ALS structurally resembles apoptosis. The progression of neuronal death is divisible into 3 sequential stages: chromatolysis, somatodendritic attrition, and apoptosis. In ALS spinal cord anterior horn and motor cortex, DNA fragmentation is detectable in situ and in gels and is internucleosomal, occurring in the presence of DNA fragmentation factor-45/40 activation and increased caspase-3 activity. By immunoblotting, changes occur in the subcellular distribution of cell death proteins that would promote apoptosis. In selectively vulnerable CNS regions in ALS compared with controls, the proapoptotic proteins Bax and Bak are elevated in the mitochondrial-enriched membrane compartment, but are reduced or unchanged in the cytosol. In contrast, the antiapoptotic protein Bcl-2 is decreased in the mitochondrial-enriched membrane compartment of vulnerable regions in ALS, but is increased in the cytosol, whereas Bcl-x_L levels are unchanged in both subcellular compartments. Coimmunoprecipitation experiments showed that Bax-Bax interactions are greater in the mitochondrial-enriched membrane compartment of ALS motor cortex compared with controls, whereas Bax-Bcl-2 interactions are lower in the membrane compartment of ALS motor cortex compared with controls. We conclude that a PCD mechanism, involving cytosol-to-membrane and membrane-to-cytosol redistribution of cell death proteins and caspase-3 activation, participates in the pathogenesis of ALS.

Key Words: Bak; Bax; Bcl-2; Bcl-x_L; Caspase; DNA fragmentation factor-45/40; Mitochondria.

INTRODUCTION

Amyotrophic lateral sclerosis (ALS) is a human disease characterized by primary degeneration of upper and lower motor neurons as well as weakness and atrophy of affected muscle (1). The mechanisms underlying the neurodegeneration in ALS are not known. Motor neuron degeneration occurs in mice with forced expression of mutant forms of the gene encoding the free radical-scavenging enzyme copper/zinc superoxide dismutase 1 (2, 3). These mutant forms of copper/zinc superoxide dismutase 1 (SOD1) have been identified in a subset (10–20%) of individuals with familial ALS (FALS) that occurs in 5–10% of patients with ALS (4, 5). This neurodegeneration is possibly related to a toxic gain in function of mutant SOD1 (2, 6). In vitro expression of mutant SOD1 can induce neuronal apoptosis and abnormalities in the production of free radicals (6, 7). Oxidative stress resulting from down-regulation of SOD1 can also cause apoptosis in cell culture (8). Reactive oxygen species (ROS) may mediate trophic factor deprivation-induced apoptosis of sympathetic neurons in vitro (9) and target deprivation-induced apoptosis of central neurons in vivo (10). Because motor neuron survival depends on trophic factors (11, 12), abnormalities in neurotrophin support may result in apoptotic death of motor neurons in ALS by inducing a PCD mechanism involving the generation of ROS. This hypothesis is supported indirectly by experiments showing oxidative damage in CNS tissues of ALS subjects (13, 14) and abnormalities in mRNA levels for Bcl-2 and Bax in spinal motor neurons in ALS (15). Furthermore, the genes for neuronal apoptosis inhibitory protein and survival motor neuron protein are either deleted partially or are mutant in children with spinal muscular atrophy (16, 17), a pediatric form of motor neuron disease.

However, it still has not been shown if neuronal apoptosis contributes to the neurodegeneration in ALS. Subsets of neurons in individuals with ALS undergo nuclear DNA fragmentation, as determined by in situ end-labeling of DNA strand breaks (18, 19, 20), but this method does not distinguish between apoptotic and necrotic cell deaths (21, 22). Therefore, in this study, we examined the neuronal death in postmortem cases of ALS with respect to cell structure and DNA fragmentation patterns to determine whether degenerating motor neurons have an apoptotic phenotype, as compared with known paradigms of neuronal apoptosis in the CNS (21–26). Because PCD is a mechanism for apoptosis (22), we also tested the hypothesis that changes occur in the expression or activity of proteins that function in PCD in selectively vulnerable CNS regions in ALS.

MATERIALS AND METHODS

Subjects

Patients were diagnosed as having ALS by clinical and neuropathological criteria (1). Only 1 (case 1176) of 15 cases studied here met the criteria for the diagnosis of FALS; the other cases were diagnosed as sporadic ALS (Table 1). CNS tissues

From the Departments of Pathology, Division of Neuropathology, and Neuroscience, Johns Hopkins University School of Medicine, Baltimore, Maryland.

Correspondence to: Lee J. Martin, PhD, Johns Hopkins University School of Medicine, Department of Pathology, 720 Rutland Avenue, 558 Ross Building, Baltimore, MD 21205–2196.

This research was supported by a grant from the US Public Health Service (NS 34100).

TABLE 1
Control and ALS Cases Evaluated

Group	Case number	Age (yr)/Sex	Postmortem delay (h)	Cause of death
Control	487	73/male	22	Pancreatic adenocarcinoma
	515	62/male	21	Aortic aneurysm
	712	44/female	20	Pneumonia
	719	66/male	10	Myocardial infarction
	961	59/female	6	Myocardial infarction
	993	66/male	12	Prostatic carcinoma
ALS	345	59/female	3	Respiratory arrest
	414	65/male	4	Respiratory arrest
	433	71/male	17	Respiratory arrest
	447	69/female	15	Respiratory arrest
	492	68/female	18	Respiratory arrest
	834	46/male	3	Respiratory arrest
	875	70/female	24	Respiratory arrest
	950	38/male	22	Respiratory arrest
	1014	72/male	5	Respiratory arrest
	1088	66/male	7	Respiratory arrest
	1108	64/female	8	Respiratory arrest
	1151	57/female	14	Respiratory arrest
	1161	47/male	6	Pneumonia
	1169	67/female	15	Respiratory arrest
	1176	27/male	6	Respiratory arrest
	1485	61/female	5	Respiratory arrest

were obtained from the Human Brain Resource Center, Division of Neuropathology, Johns Hopkins University School of Medicine. Postmortem samples of brain and spinal cord from age-matched control individuals without neurological disease (n = 6) and patients with either sporadic ALS or FALS (n = 16) were selected randomly for analysis (Table 1). The mean ages for control and ALS groups were 62 ± 10 yr and 59 ± 13, respectively. The postmortem delays of the 2 groups were comparable (15 ± 7 h and 11 ± 7 h for control and ALS groups, respectively).

Neuropathology

Paraffin-embedded blocks of spinal cord (cervical, thoracic, and lumbar), brain stem, striatum, precentral gyrus (motor cortex), and postcentral gyrus (somatosensory cortex) were sectioned (10 μm) and stained with hematoxylin and eosin (H&E). Adjacent sections were stained with the TUNEL method, as described (21), and were counterstained with cresyl violet to identify neurons undergoing nuclear DNA fragmentation. In addition, samples of anterior horn were micropunched from formalin-fixed spinal cords of control and ALS cases, immersed in 2% glutaraldehyde for 72 h, and embedded in plastic. Anterior horn samples were cut at 1 μm and stained with toluidine blue for higher resolution light microscopic analyses.

DNA Gel Electrophoresis

Because the TUNEL method identifies dying neurons irrespective of cell death mechanisms (21, 22), DNA fragmentation patterns were examined in agarose gels to detect random digestion (necrotic) and/or internucleosomal cleavage (apoptotic) of DNA. Genomic DNA was isolated from micropunches of spinal cord anterior horn, motor cortex, and somatosensory cortex from control (n = 3) and ALS (n = 6) cases. Tissue samples were homogenized in DNA extraction buffer containing 10 mM Tris (pH 7.4), 10 mM NaCl, 25 mM EDTA, 1% SDS, and 1 mg/ml proteinase K and were incubated in the same buffer overnight at 37°C. DNA was extracted with an equal volume of salt saturated-phenol: chloroform: isoamyl alcohol (10:10:1) and the recovered aqueous phase was extracted with diethyl ether. DNA was precipitated with ethanol (2.5 volumes). The DNA pellet was dissolved in 0.1X SSC and incubated (37°C) with DNase-free RNase A (0.1 mg/ml) for 1 h, and then overnight (37°C) with 0.1 mg/ml proteinase K. DNA was re-extracted, precipitated, and dissolved in TE buffer. DNA samples (~1.0 μg) were 3'-end labeled with digoxigenin-11-ddUTP using terminal transferase (Boehringer Mannheim), precipitated, resuspended in TE buffer, fractionated by agarose gel (1.2%–1.5%) electrophoresis, and transferred to nylon membrane followed by UV-cross-linking. Membranes were incubated in 2% nucleic acid blocking reagent (Boehringer Mannheim) and then in blocking reagent containing 75 mU/ml antidigoxigenin Fab fragments conjugated to alkaline phosphatase (Boehringer Mannheim). After washing, membranes were reacted with CSPD detection reagent (Boehringer Mannheim) and exposed to Kodak X-OMAT film to visualize DNA.

Immunoblotting

Samples from the motor cortex (superior precentral gyrus, leg area), somatosensory cortex, and spinal cord were used for immunoblotting. Using 4 or 2 mm diameter micropunches (Acuderm Inc., Fort Lauderdale, FL), neocortical samples (0.3–

TABLE 2
Cell Death Proteins Analyzed

Antibody	Source	Amino acid epitope*	Immunoblot dilution
α-DFF-45/40	Zymed	N-terminus	500 ng/ml
α-Bak	Santa Cruz (G-23)	82–104	200 ng/ml
α-Bak	Upstate	23–37	1 μg/ml
α-Bax	Santa Cruz (P-19)	43–61	200 ng/ml
α-Bax	Santa Cruz (N-20)	11–30	200 ng/ml
α-Bax	Upstate	1–21	2 μg/ml
α-Bax	PharMingen (6A7)	12–24	1 μg/ml
α-Bcl-2	Santa Cruz (N19)	4–21	200 ng/ml
α-Bcl-2	Dako (clone 124)	41–54	200 ng/ml
α-Bcl-x_L	Oncogene	261–277	1:4,000

* All antibodies were generated against amino acid sequences in human proteins, except the P-19 α-Bax, which was generated against the mouse sequence.

0.5 g) and segmental samples (0.1–0.3 g) were obtained from fresh-frozen postmortem brain slabs of the right hemisphere or from the spinal cord that were stored at −70°C and warmed to −20°C. Samples of spinal cord included only the anterior horn gray matter (mostly the group IX column) of cervical or lumbar levels. Samples were homogenized with a Brinkman Polytron in cold 20 mM Tris HCl (pH 7.4) containing 10% (wt/vol) sucrose, 20 U/ml aprotinin (Trasylol), 20 μg/ml leupeptin, 20 μg/ml antipain, 20 μg/ml pepstatin A, 20 μg/ml chymostatin, 0.1 mM phenylmethylsulfonyl fluoride, 10 mM benzamidine, 1 mM EDTA, and 5 mM EGTA. Crude homogenates were centrifuged at 1,000 g_{av} for 10 min. The supernatant (S1 fraction) was then centrifuged at 114,000 g_{av} for 20 min. The resulting supernatant (S2 soluble fraction) was collected, and the pellet (P2 mitochondrial-enriched, membrane fraction) was washed in homogenization buffer (without sucrose) 3 times by resuspension, each followed by centrifugation at 114,000 g_{av} for 20 min. The washed membrane fraction was resuspended fully in this buffer supplemented with 20% (wt/vol) glycerol. Protein concentrations in soluble and membrane fractions were measured by a Bio-Rad protein assay with bovine serum albumin as a standard.

The levels of Bcl-2, Bcl-x_L, Bax, and Bak immunoreactivity were quantified by immunoblotting using antibodies purchased from commercial sources (Table 2). In addition, we evaluated the cleavage of DNA fragmentation factor (DFF-45/40), which is a caspase-3 target protein that causes internucleosomal cleavage of DNA and chromatin condensation in human cells during apoptosis (27). Samples of membrane or soluble proteins from ALS and control cases were subjected to 15% sodium dodecyl sulfate polyacrylamide gel electrophoresis (SDS-PAGE) and transferred to nitrocellulose membrane by electroblotting. Positive controls for cell death proteins included human A431cell (epidermal carcinoma) lysates for Bak, rat intestine for Bax, rat thymus or intestine for Bcl-2, and HeLa cell lysates for Bcl-x_L. The reliability of sample loading and electroblotting in each experiment was evaluated by staining nitrocellulose membranes with Ponceau S before immunoblotting, and by reprobing blots with antibody to synaptophysin (p38), an integral synaptic vesicle membrane protein (28). Blots were blocked with 2.5% nonfat dry milk with 0.1% Tween 20 in 50 mM Tris-buffered saline (pH 7.4), then incubated overnight at 4°C with antibody (Table 2). After the primary antibody incubation, blots were washed and incubated with peroxidase-conjugated secondary antibody (0.2 μg/ml) and developed with enhanced chemiluminescence (Amersham).

To identify protein interactions among Bax and Bcl-2 in human CNS samples and possible abnormalities in these protein interactions in ALS, immunoprecipitation experiments were performed. Mitochondrial-enriched fractions (50-μg protein) were reacted overnight with antibodies to Bax or Bcl-2. Immunocomplexes were captured with protein A-agarose bead slurry, washed, and subjected to SDS-PAGE for subsequent analysis by western blotting. Negative control experiments, Bax and Bcl-2 antibodies were neutralized with synthetic peptides corresponding to sequences within the molecules (10-μg peptide/1 μg antibody).

To quantify cell death protein immunoreactivity, films were scanned using a Macintosh Adobe Photoshop program and an Agfa Arcus Plus scanner. Densitometric analysis was performed using signal Analytics IP Lab Gel software. Protein levels were expressed as relative optical density measurements, determined by comparing the density and area of the immunoreactive bands from ALS cases with corresponding bands in control lanes in the same blot. The values for each case and the group means and variances were replicated in triplicate or quadruplicate experiments. Because the assumptions for parametric analyses were not violated (i.e. the sample populations were selected randomly and were normally distributed), analysis of changes in cell death proteins by quantitative immunoblotting was performed by comparison of age-matched control values with ALS values by one-way analysis of variance, and subsequent statistical evaluations for significance were made using a 2 sample Student's *t*-test.

Caspase-3 Activity Assay

The biochemical activity of caspase-3 in CNS tissue samples from ALS and control cases (Table 1) was measured using a colorimetric assay (R&D Systems, Minneapolis, MN). Micropunched samples of spinal cord anterior horn (0.1–0.4 g, n = 3 controls and n = 10 ALS), motor cortex (0.2–0.7 g, n = 3 controls and n = 6 ALS), and somatosensory cortex (0.2–0.6 g, n = 2 controls and n = 4 ALS) were homogenized in cell lysis buffer, and protein concentrations were measured by a Bio-Rad protein assay with bovine serum albumin as a standard. The assay was performed using 200 or 300 μg of total protein and DEVD (Asp-Glu-Val-Asp)-pNA as caspase-3 colorimetric substrate in a reaction volume of 50 or 100 μl incubated 2–4 h at 37°C. After the incubation, the reaction mixture was centrifuged at 14,000 rpm for 5 min, and the absorbance of the supernatant was measured spectrophotometrically at 405 nm. The negative controls for this assay were reactions without homogenate, reactions without substrate, and reactions with homogenate and substrate in the presence of the caspase-3 inhibitor Ac-DEVD-CHO (Alexis Biochemicals, San Diego, CA). The results were replicated in triplicate experiments and were evaluated for significance using analysis of variance followed by a Student's *t*-test.

RESULTS

Motor Neuron Degeneration in ALS Is Structurally Apoptotic

The morphology of motor neuron degeneration in the spinal cord of ALS cases was examined by light microscopy to determine if it structurally resembles apoptosis, as found in in vivo paradigms of neuronal apoptosis (21–26). Criteria for identifying cells as motor neurons included size, shape, and aggregates of Nissl substance. By arranging motor neurons at different stages of degeneration in H&E sections (Fig. 1) and in semithin plastic sections (Fig. 2) of spinal cord, a staging scheme was formulated for the structural progression of neuronal death. This staging arrangement reveals that motor neuron degeneration in ALS resembles apoptosis. After an initial chromatolytic stage (Fig. 1B), motor neurons progressively undergo attrition of the cell body and dendrites (Fig. 1C–H) that culminates in residual motor neurons of only ~20% of normal diameter (Fig. 1A, I). During the process of somatodendritic attrition, both the cytoplasm and the nucleus become condensed and dark (Fig. 1), consistent with apoptosis in neurons (21–26). This cytoplasmic and nuclear condensation of motor neurons was verified in 1-μm-thick plastic sections of anterior horn micropunches (Fig. 2). Plastic sections also revealed the absence of appreciable vacuolar and edematous cytopathology in motor neurons in the various stages of degeneration in ALS (Fig. 2). However, the nuclear condensation in ALS motor neurons (Fig. 2) differed from classical apoptosis because the chromatin was not discretely organized into uniformly round, dense clumps as in animal models of neuronal apoptosis (21, 22, 25, 26).

Degenerating Motor Neurons Undergo Nuclear DNA Fragmentation Which Is Associated With Internucleosomal Cleavage of DNA and Elevated Levels of DNA Fragmentation Factor-40

The TUNEL method was used to identify when nuclear DNA fragmentation commences during the staging of motor neuron degeneration in ALS (Fig. 3). DNA fragmentation was detected in motor neurons at the somatodendritic attrition (Fig. 3B) and apoptotic (Fig. 3C, D) stages of neuronal death, but not in motor neurons in the chromatolytic stage of degeneration (Fig. 3A). DNA fragmentation was also found in subsets of pyramidal neurons in ALS motor cortex, but not somatosensory cortex (data not shown). All paraffin sections of cervical and lumbosacral spinal cord of ALS cases contained TUNEL-positive motor neurons. In 400× microscopic fields with TUNEL-positive motor neurons, the number of labeled motor neurons ranged from 1 to 6 cells per field. DNA fragmentation in degenerating motor neurons persists throughout the apoptotic stage of cytoplasmic and nuclear condensation and cell shrinkage (Fig. 3C, D). Subsets of non-neuronal cells (glial and possibly hematogenous-derived) were also TUNEL-positive (Fig. 3E). However, labeling of non-neuronal cells was found in controls and in cases of ALS (as many as 6–10 cells/400× field) in contrast to the labeling of motor neurons, which was specific for ALS. TUNEL-positive non-neuronal cells were also found in the striatum of ALS cases (not shown). Counts of TUNEL-positive non-neuronal cells revealed values in ALS spinal cord and motor cortex that were 134% ± 28% (mean ± SD) of control. Therefore, the majority of TUNEL positivity associated with non-neuronal cells was thought to be related to postmortem autolysis, consistent with previous studies advocating cautious interpretation of TUNEL positivity in human postmortem brain (29).

By gel electrophoresis (Fig. 4), an internucleosomal pattern of DNA fragmentation indicative of PCD was detected in samples of DNA extracted from micropunches of spinal cord anterior horn and motor cortex of ALS cases. Internucleosomal DNA fragmentation was not detected in somatosensory sensory cortex of ALS cases nor was internucleosomal DNA fragmentation detected in spinal cord anterior horn and neocortex of age- and postmortem delay-matched controls (Fig. 4). In some cases with prolonged postmortem intervals, a ladder pattern coexisted with random DNA degradation in ALS cases and a faint smear pattern could be detected in control cases (depending on the concentration of agarose gel used).

To identify an upstream molecular pathway that could be responsible for the internucleosomal fragmentation of DNA found in ALS, we determined by immunoblotting whether the enzyme responsible for internucleosomal fragmentation of DNA is activated in ALS. DFF-40, the 40 kDa active enzyme for internucleosomal DNA cleavage and chromatin condensation (27), was detected at high levels in cytosolic fractions of motor cortex and spinal cord anterior horn of ALS cases compared with controls (Fig. 5).

Caspase-3 Activity Is Elevated in ALS

The cleavage of DFF-45/40 is caused by caspase-3 (27); therefore we measured the activity of caspase-3 in human CNS. Colorimetric determination of caspase-3 activity revealed regionally specific increases in enzyme activity in ALS cases compared with age- and postmortem delay-matched controls. In the presence of 25 μM Ac-DEVD-CHO, caspase-3 activity in human CNS homogenates was inhibited ~85% (data not shown), confirming the specificity of this assay. Caspase-3 activity in ALS anterior horn was 115% ± 28% (mean ± SD) of control. In ALS neocortex, caspase-3 activity was significantly ($p < 0.05$) increased to 210% ± 37% of control in motor cortex, but was not changed in somatosensory cortex (103% ± 13%).

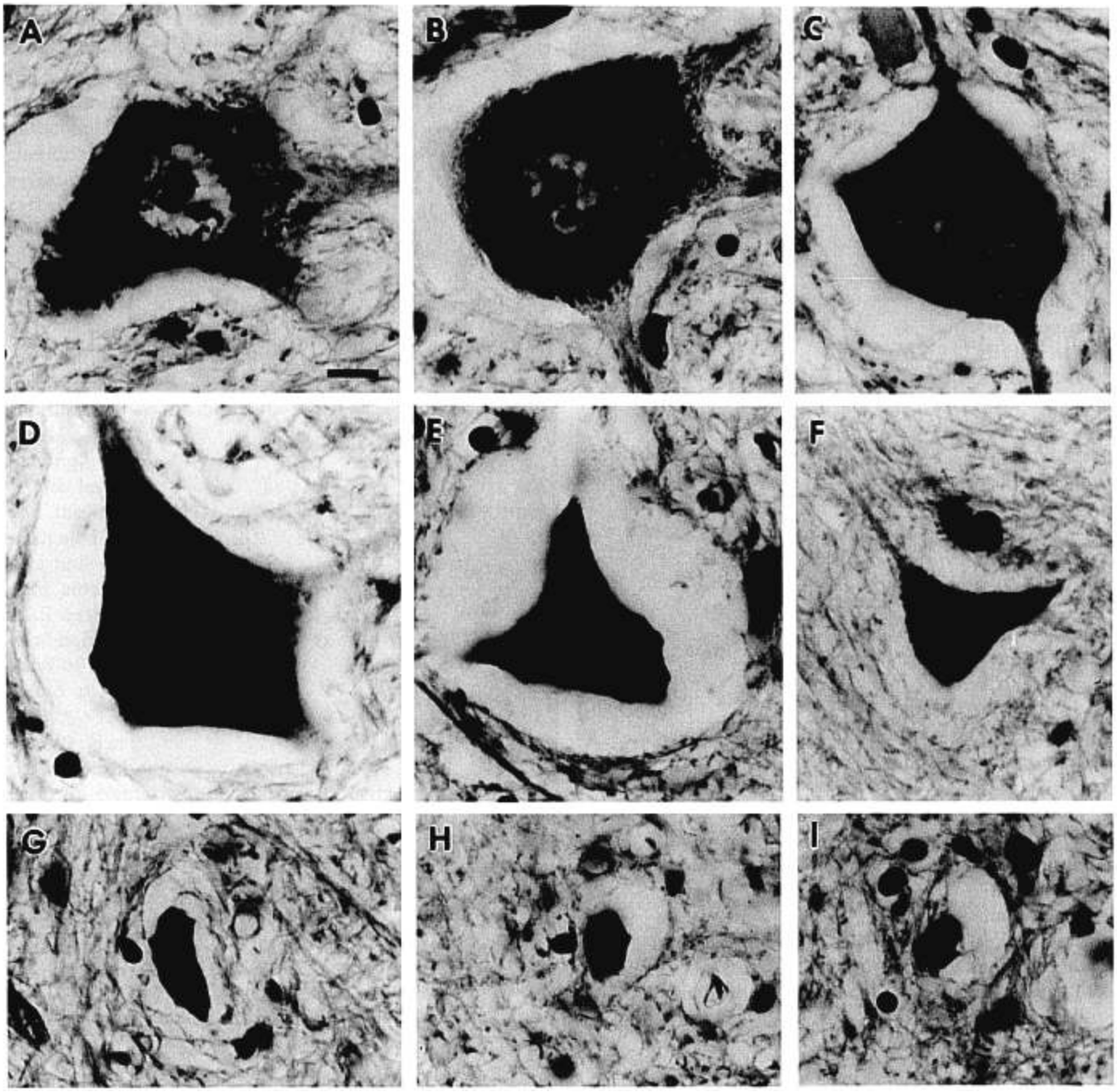

Fig. 1. Motor neuron degeneration in ALS can be classified according to a morphological staging scheme. H&E-stained paraffin sections (10-μm-thick) of lumbar spinal cord were used to arrange motor neurons at different stages of degeneration into a staging sequence showing a possible morphological progression for neurodegeneration. A normal motor neuron (A) from a control subject is shown for comparison with motor neurons from subjects with ALS (B–I). Three major structural stages of degeneration can be identified: chromatolysis (B, C), somatodendritic attrition (D–F), and apoptosis (G–I). A subset of motor neurons can be found in chromatolysis as characterized by dispersed Nissl substance and an eccentrically located nucleus with the cell body appearing swollen and round (B, C). Some chromatolytic neurons have prominent cytoplasmic hyaline body inclusions (C). The transition between chromatolytic and attritional stages is characterized by the onset of cytoplasmic and nuclear basophilia. During the attritional stage (D–F), the cytoplasm and nucleus become homogeneously dark and condensed and the cell shrinks, progressively loosing the multipolar shape. Affected motor neurons appear to spend most of the time in the attritional stage. At the apoptotic stage (G–I), motor neurons assume a highly shrunken and condensed morphology and typically have a fusiform or round residual shape. Scale bar in A = 11 μm (same for B–I).

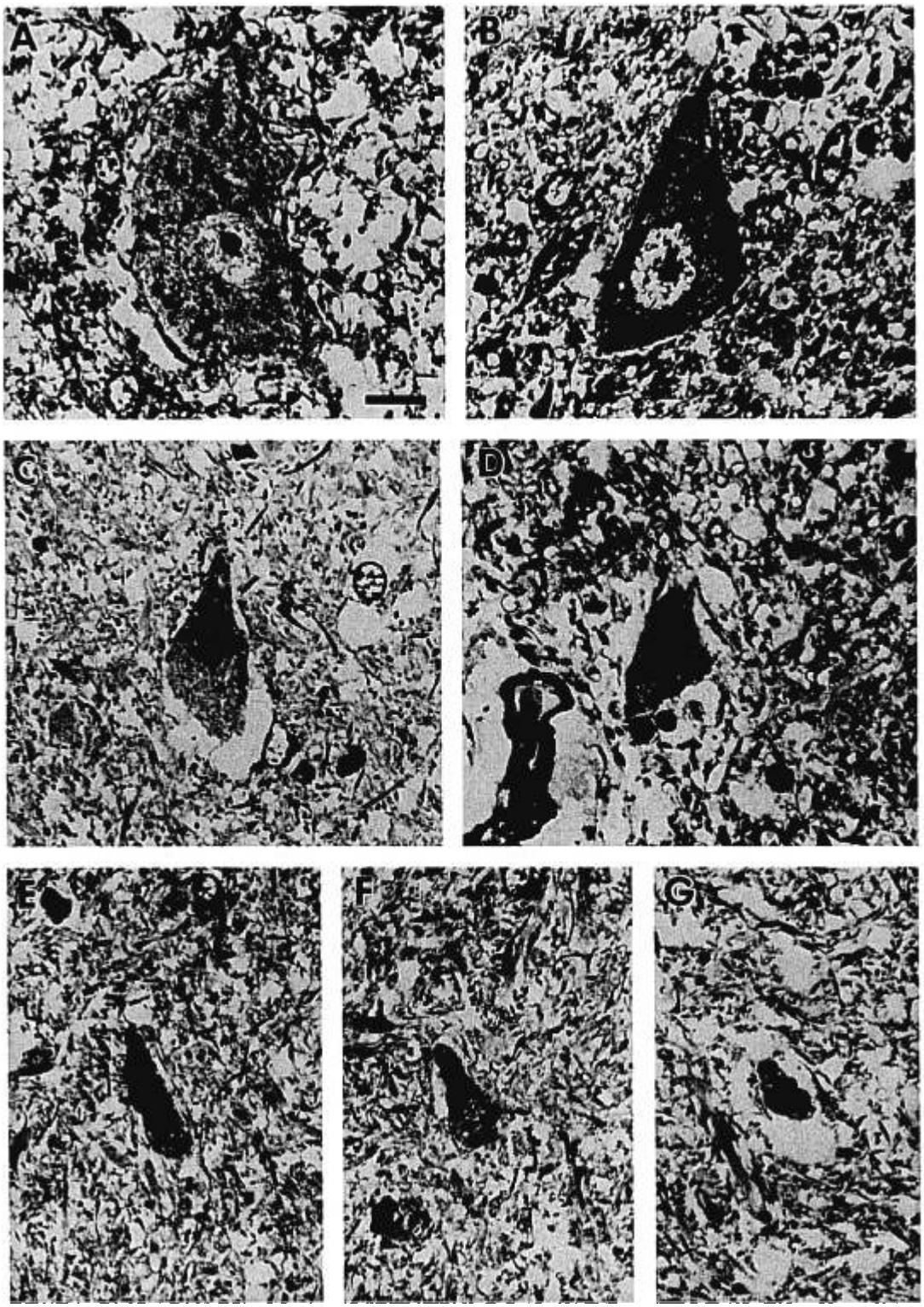

Fig. 2. Motor neuron degeneration resembles apoptosis. The possible progression of structural changes in the cytoplasm and nucleus of degenerating motor neurons in ALS is shown in plastic sections (1-μm-thick). A normal motor neuron with large Nissl bodies (A) from a control subject is shown for comparison with motor neurons from subjects with ALS (B–G). The 3 major morphological stages of degeneration are shown: chromatolysis (B), somatodendritic attrition (C, D), and apoptosis (E–G). The chromatolytic neuron (B) shows dispersion of large Nissl bodies and redistribution of remaining Nissl substance to the cell periphery. In the chromatolytic stage, the nucleus is not yet condensed. Compare B with cells at the same stage of degeneration shown in Figure 1B, C. In the attritional stage (C, D), the nucleus becomes progressively dark and condensed, but the nucleolus is still apparent, as the cytoplasm becomes more homogeneous in appearance. Compare C and D with cells at the same stage of

Subcellular Alterations in PCD Proteins Occur in ALS

The extent of cross-contamination between proteins in subcellular fractions was assessed by assaying for either the cytosolic enzyme marker lactate dehydrogenase or the mitochondrial enzyme cytochrome c oxidase. The mitochondrial enrichment of membrane fractions was verified by immunoblot analysis using antibodies to subunit I of cytochrome c oxidase (Molecular Probes); in contrast, cytochrome c oxidase subunit I was not detected in cytosolic fractions, but these fractions were enriched in lactate dehydrogenase (data not shown). Synaptophysin (p38), a 38-kDa integral membrane protein found in synaptic vesicles of nerve terminals (28), was also enriched in mitochondrial-enriched membrane fractions, but not in cytosolic fractions. Synaptophysin levels did not change significantly in ALS regions compared with controls (Figs. 6, 7); thus, p38 was used as an index of protein loading.

The levels of the proapoptotic proteins Bax and Bak and the antiapoptotic proteins Bcl-2 and Bcl-x_L were evaluated in membrane fractions enriched in mitochondria and in cytosolic fractions of motor cortex, spinal cord anterior horn, and somatosensory cortex from 16 ALS cases and 6 control cases (Table 1). In mitochondrial-enriched membrane and soluble fractions, a major band of protein that reacted with Bax antibodies was detected at ~21 kDa, consistent with the molecular mass of Bax-α (30, 31). The ~21 kDa Bax monomer was present at higher levels in the cytosolic compartment as compared with the membrane fraction in control human CNS (Fig. 6). Neutralization of Bax antibodies with synthetic peptide antigen corresponding to an amino acid sequence mapping at the amino terminus of human Bax blocked the detection of immunoreactivity in these subcellular fractions (data not shown). Immunoreactivity for Bak in human CNS was detected at ~29 kDa, consistent with other results (32). In normal human CNS, Bak was found at much higher levels in the mitochondrial-enriched membrane compartment as compared with the cytosolic compartment (Fig. 6). Bax and Bak were increased (146% and 156%, respectively) in mitochondrial-enriched membrane fractions of ALS motor cortex compared with controls (Fig. 6; Table 3). Bax and Bak were also increased (346% and 162%, respectively) in membrane fractions of ALS spinal cord compared with controls (Fig. 7; Table 3). Bax and Bak levels were unchanged in membrane fractions of ALS somatosensory cortex (Table 3). In contrast to the increases in Bax and Bak in mitochondrial-enriched membrane fractions, the levels of these proapoptotic proteins were either decreased or unchanged in the cytosol (Fig. 6; Table 3).

Bcl-2 and Bcl-x_L were differentially expressed in the human CNS. Antibodies to Bcl-2 reacted with a major band of proteins in subcellular fractions of human CNS that migrated at ~26 kDa (Fig. 6). In control human CNS, Bcl-2 is found at higher levels in the membrane compartment as compared with the cytosolic compartment (Fig. 6). Antibodies to Bcl-x_L reacted with a major band of proteins in subcellular fractions of human CNS that migrated at ~29 kDa. Bcl-x_L is enriched in both mitochondrial-enriched membrane and cytosolic compartments (Fig. 6). In the adult human CNS, Bcl-x_L is expressed at much higher levels compared with Bcl-2 (Fig. 6). These results are consistent with other data on Bcl-2 (33, 34) and Bcl-x_L (35, 36). Neutralization of Bcl-2 antibodies with synthetic peptide antigen corresponding to an amino acid sequence mapping at the amino terminus of human Bcl-2 blocked the detection of the 26-kDa-immunoreactive band (data not shown). Bcl-2 levels were decreased in the mitochondrial-enriched membrane compartment in ALS motor cortex (43% of control) and spinal cord (34% of control), but not in sensory cortex (Figs. 6, 7; Table 3). In contrast, Bcl-2 levels were increased markedly in the cytosolic fractions of ALS motor cortex (Fig. 6) and spinal cord compared with control (Table 3). Bcl-x_L protein levels did not change significantly ($p < 0.05$) in mitochondrial-enriched membrane fractions or cytosolic fractions of ALS motor cortex and spinal cord (Figs. 6, 7; Table 3)

Immunoprecipitation experiments were conducted to identify Bax-Bax and Bax-Bcl-2 interactions in human CNS tissues and to identify possible differences in these protein interactions in ALS versus control motor cortex (Fig. 8). In mitochondrial-enriched membrane fractions of motor cortex, Bax-Bax associations were increased in ALS cases (180% ± 32% of control, mean ± SD), and Bax-Bcl-2 interactions were reduced in ALS cases (74% ± 12% of control, mean ± SD).

DISCUSSION

These experiments were undertaken to further understand the mechanisms for neurodegeneration in ALS. Our results indicate that the neuronal degeneration in ALS occurs by a PCD mechanism and that this pathway for cell death appears to have a major contribution to the pathogenesis of ALS. This conclusion is based on the

←

degeneration shown in Figure 1D–F. Motor neurons in the apoptotic stage (E, F) are highly shrunken and without dendrites. At endstage apoptosis (G), residual motor neurons contain a small, pyknotic nucleus surrounded by a sparse rim of condensed cytoplasm. Motor neurons at endstage degeneration may represent a single apoptotic body for this type of neuron in the adult CNS. Compare E–I with similar cells in Figure 1G–I. Scale bar in A = 11 μm (same for B–G).

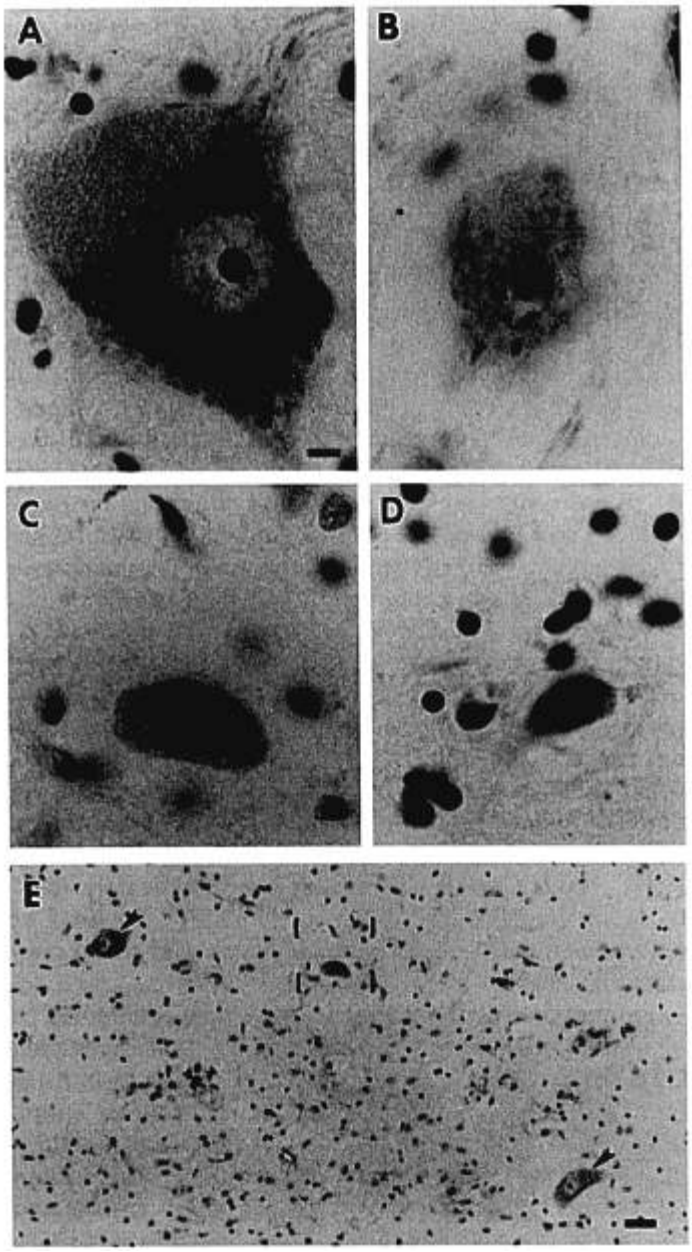

Fig. 3. TUNEL demonstrates that motor neurons in ALS undergo DNA fragmentation during the attritional and apoptotic stages of degeneration, but not at the chromatolytic stage. TUNEL preparations for visualizing DNA fragmentation in situ (brown labeling within the nucleus) were counterstained with cresyl violet to show Nissl substance. During chromatolysis (A), motor neurons (characterized by dispersed Nissl substance and an eccentrically located nucleus) do not undergo DNA fragmentation. Scale bar in A = 5 μm (same for B–D). During the stage of somatodendritic attrition (B), degenerating motor neurons become TUNEL-positive, with the nucleolus showing prominent labeling. During the apoptotic stage (C, D), the condensed nucleus within degenerating motor neurons is intensely TUNEL-positive. A panoramic view shows (E) that this DNA fragmentation occurs in isolated motor neurons (neuron in brackets is shown in C), but not in nearby motor neurons (arrowheads). Scale bar in E = 57 μm.

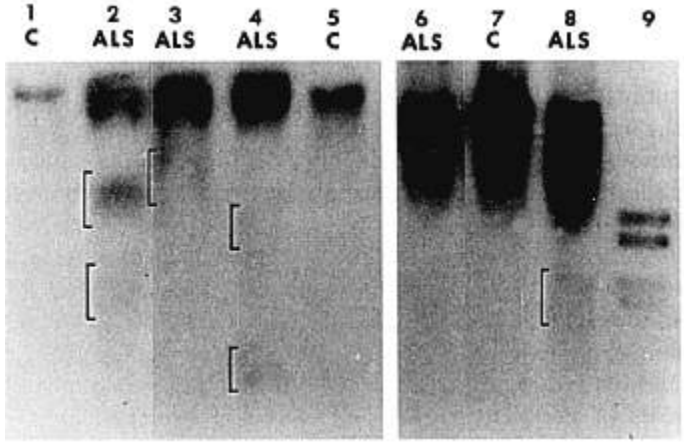

Fig. 4. Gel electrophoretic analysis of DNA fragmentation patterns in ALS and control (C) spinal cord anterior horn (lanes 1–5), somatosensory cortex (lane 6), and motor cortex (lanes 7 and 8). Base pair molecular weight markers (lane 9) are (top to bottom): 2176, 1766, 1230, and 1033. Brackets identify internucleosomal fragments observed in ALS spinal cord (lanes 2, 3 and 4) and motor cortex (lane 8). No internucleosomal fragmentation was detected in ALS somatosensory sensory cortex (lane 6) or in control spinal cord (lanes 1 and 5) and control motor cortex (lane 7).

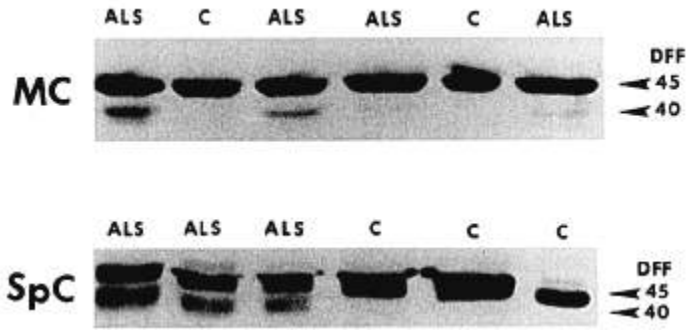

Fig. 5. Immunoblot analysis of DFF-45/40 in ALS and control (C) motor cortex (MC) and spinal cord (SpC) cytosolic fractions. Samples were fractionated in 15% gels (MC) or 10% gels (SpC). The 45-kDa DFF protein was detected in cytosolic fraction of both control and ALS cases at comparable levels, whereas the 40 kDa DFF subunit (the active DFF) was found in ALS.

structure of motor neuron degeneration, the patterns of DNA fragmentation, the formation of the active 40 kDa subunit of DFF, the increased caspase-3 activity, and on the subcellular abnormalities in the levels of proapoptotic (Bax and Bak) and antiapoptotic (Bcl-2) proteins in selectively vulnerable regions in individuals with ALS. Neuronal death in ALS appears to be a form of apoptosis and is asynchronous, as indicated by the ability to formulate a cytopathological staging scheme in which motor neurons are found at various stages of degeneration ranging from chromatolysis to near endstage apoptosis. This interpretation is consistent with the clinical progression of the disease (1). In addition, our TUNEL observations,

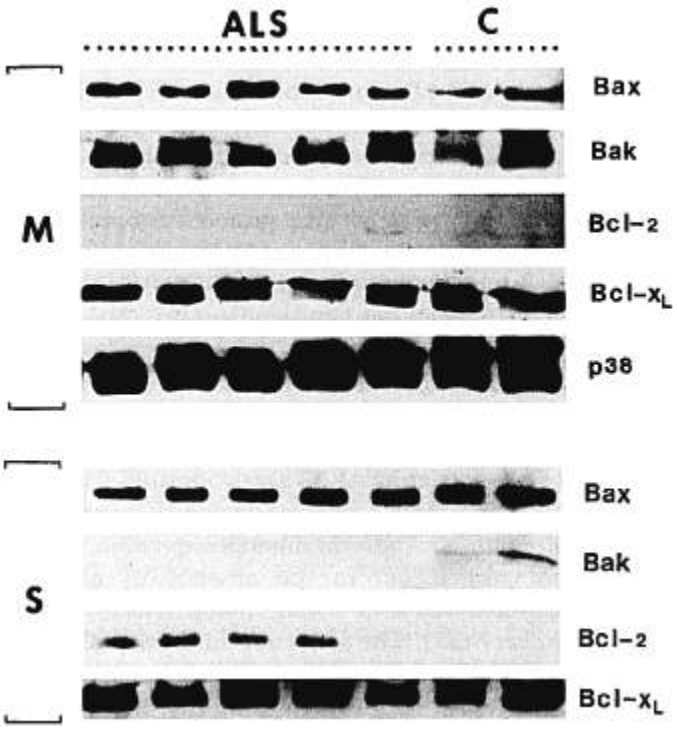

Fig. 6. Immunoblot analysis of proapoptotic (Bax and Bak) and antiapoptotic (Bcl-2 and Bcl-x_L) protein levels in mitochondrial-enriched membrane fractions (M) and soluble/cytosolic fractions (S) of motor cortex from individuals with ALS and age-matched controls (C). For membrane fractions, synaptophysin (p38) was used as a control for protein loading. Longer exposures revealed darker bands of immunoreactivity for Bcl-2 in membrane and soluble compartments and darker bands of immunoreactivity for Bak in the soluble compartment. In these situations the darker exposures were used for quantification.

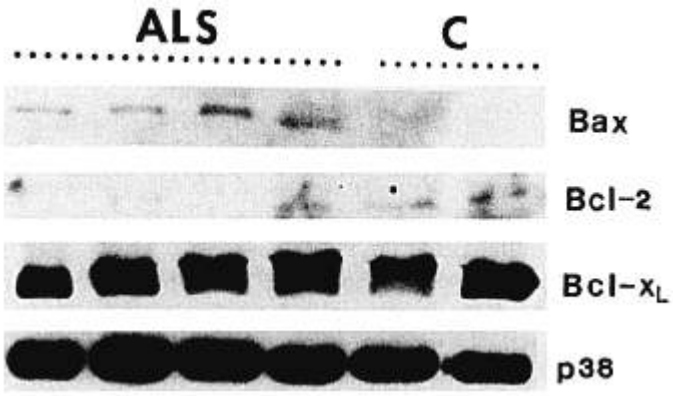

Fig. 7. Immunoblot analysis of proapoptotic (Bax) and antiapoptotic (Bcl-2 and Bcl-x_L) protein levels in mitochondrial-enriched membrane fractions of spinal cord anterior horn from ALS and controls (C). Synaptophysin (p38) was used as a control for protein loading.

and those in other studies (18, 19, 20), reveal that neuronal death, as shown by nuclear DNA fragmentation, is ongoing at a significant magnitude in individuals with ALS, even at the time of death. Our experiments demonstrating internucleosomal cleavage of DNA and abnormalities in the expression of cell death proteins in both motor cortex and spinal cord is consistent with the conclusion that apoptosis of upper and lower motor neurons in ALS is an ongoing structural and molecular process that is contributing to the pathogenesis of this disease. The processing of DFF-45/40 suggested that caspase-3 is abnormally activated in ALS, and the biochemical analysis of caspase-3 activity directly confirmed this conclusion, thereby providing a mechanism for the internucleosomal fragmentation of DNA found in ALS. Thus, despite our analysis of postmortem human CNS tissues at endstage disease, these results provide important information about the mechanisms for neuronal degeneration in ALS.

Our strategy for sampling postmortem CNS tissues from ALS and control cases is possibly relevant to the outcome of these experiments. Discrete micropunches of gray matter were used, rather than large pieces of nervous tissue indiscriminate of gray and white matter. For spinal cord, highly selective micropunches of anterior horn gray matter were used to minimize contamination of sensory horn and surrounding white matter. This discriminating microdissection approach may have aided in the detection of internucleosomal DNA fragmentation, caspase-3 activation, and regional differences in the levels of Bax, Bak,

TABLE 3
Immunoblot Analysis of Cell Death Protein Levels in ALS

	Motor cortex		Spinal cord (anterior horn)		Sensory cortex
	Membrane	Cytosolic	Membrane	Cytosolic	Membrane
Bax	146 ± 19*	72 ± 12*	346 ± 45*	115 ± 22	123 ± 10
Bak	156 ± 28*	21 ± 3*	162 ± 19*	69 ± 34	118 ± 13
Bcl-2	43 ± 14*	320 ± 76*	34 ± 9*	222 ± 7*	103 ± 16
Bcl-x_L	82 ± 12	72 ± 19	130 ± 34	79 ± 12	84 ± 24

All values are % of control (mean ± SD). Asterisk indicates significant difference ($p < 0.05$) from control. Sixteen ALS cases and 6 control cases were evaluated.

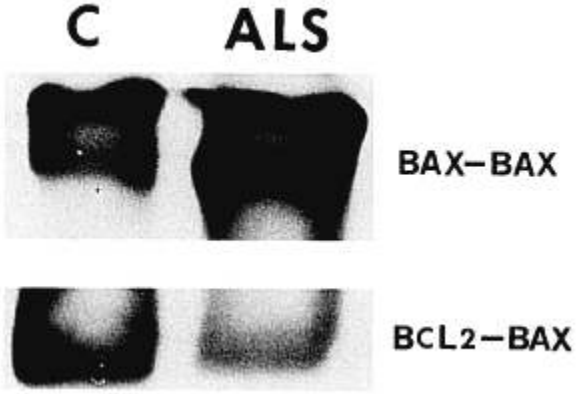

Fig. 8. Immunoprecipitation reveals abnormalities in the interactions among Bcl-2 family members in ALS brain. Equal amounts of motor cortical mitochondrial-enriched membrane fractions (50 μg protein) from control (C) and ALS cases were used to immunoprecipitate Bax with Bax monoclonal antibody followed by western analysis with Bax polyclonal antibody (upper gel), or samples were immunoprecipitated with Bcl-2 monoclonal antibody followed by western analysis with Bax polyclonal antibody (lower gel). Bax-Bax interactions were greater in samples of ALS motor cortex compared with control. In contrast, ALS motor cortex has less Bcl-2-Bax interactions compared with control. These results were replicated in triplicate experiments with different ALS and control cases.

and Bcl-2 proteins in cases of ALS compared with controls. These abnormalities in the expression of PCD proteins appear to correspond to the ongoing selective death of subsets of neurons, as detected by TUNEL. We used immunoblot detection of cell death proteins rather than immunohistochemical localization because the former is more conducive to quantification and because many of these commercially available antibodies (Table 2) cross-react with other proteins in CNS extracts. Also, members within the Bcl-2 family function by protein-protein interaction (31, 37), thus necessitating the analysis of these interactions by immunoprecipitation. Furthermore, some proteins of the Bcl-2 family undergo cytosol-to-membrane (e.g. Bax) or membrane-to-cytosol (e.g. Bad) translocation during apoptosis (31, 37), thus requiring the analysis of these proteins within different subcellular compartments.

In individuals with ALS, we found that Bax, Bak, and Bcl-2 protein levels were abnormal in motor cortex and spinal cord, but not in somatosensory cortex, while Bcl-x_L levels were unchanged. It is possible that dying non-neuronal cells contribute to these molecular abnormalities, but TUNEL-positive non-neuronal cells were found in cases of ALS and in controls, whereas TUNEL-positive upper and lower motor neurons were found only in cases of ALS. Thus, changes in cell death protein expression in ALS cases relative to controls would primarily reflect apoptosis in neurons. The general changes in the levels of Bax and Bcl-2 protein shown here are in accord with changes in the levels of bax and bcl-2 mRNA in ALS motor neurons (15). We also found that the functional interactions of these proteins are abnormal in ALS. Our observations on the levels of cell death proteins and the changes in their interactions in selectively vulnerable regions in ALS support the conclusion that neuronal death in ALS is structurally a form of apoptosis. Bax and Bak are cell death proteins that promote apoptosis (31, 37). Membership into the family of Bcl-2-related proteins is defined by homology domains (BH1-BH4), which function in the interactions between members. Bcl-2 family members exist as monomers, which form homo- or heterodimers and higher order multimers; for example, Bax can form homodimers or heterodimers with either Bcl-2 or Bcl-x_L (31, 37). We show here that Bax-Bax interactions are greater in ALS cases compared with controls, whereas, Bax-Bcl-2 interactions are reduced compared with controls. These immunoprecipitation experiments were carried out in the absence of nonionic detergents, which can alter configuration states of Bcl-2 family members (38). The induction of Bax or Bak expression can initiate apoptosis in the absence of any additional signal (31). The formation of Bax homodimers promotes apoptosis, whereas Bax heterodimerization with either Bcl-2 or Bcl-x_L appears to block apoptosis. Our coimmunoprecipitation experiments demonstrating more Bax-Bax interactions and less Bax-Bcl-2 interactions in the CNS of individuals with ALS as compared with controls further support the conclusion that motor neuron apoptosis in ALS may be mechanistically a form of PCD.

We show here that in mitochondrial-enriched membrane fractions of selectively vulnerable CNS regions in ALS compared with age-matched controls, Bax and Bak are increased, while Bcl-2 is decreased. In vitro studies show that membrane channels comprised of Bax (39) control the release of apoptotic protease activating factors (e.g. cytochrome c) from mitochondria into the cytosol (40, 41). The antiapoptotic proteins Bcl-2 and Bcl-x_L block the release of cytochrome c from mitochondria (42, 43) and thus the activation of caspase-3 and its target proteins, such as DFF-45/40 which causes internucleosomal fragmentation of DNA and chromatin condensation (27, 44). The blockade of cytochrome c release from mitochondria by Bcl-2 and Bcl-x_L is possibly due to the inhibition of Bax channel-forming, proapoptotic activity in the outer mitochondrial membrane (39) or to the regulation of mitochondrial membrane potential and volume homeostasis (45). The changes that occur in the levels of cell death proteins in mitochondrial-enriched membrane fractions of individuals with ALS would favor the activation of a caspase-dependent apoptotic mechanism as described in in vitro model systems (27, 40, 41, 45).

In cultured cells undergoing apoptosis, Bax moves from the cytosol to mitochondrial membranes (31, 46, 47). In ALS, we show that both Bax and Bak undergo a

cytosol-to-membrane redistribution with these proapoptotic proteins abnormally accumulating in mitochondrial-enriched cell membrane extracts. At the same time, Bcl-2 undergoes a membrane-to-cytosol redistribution in individuals with ALS, suggesting that Bcl-2 is abnormally released from intracellular membranes into the cytosol or is inefficiently targeted to organelle membranes, where Bcl-2 is thought to exert its antiapoptotic functions at major intracellular sites of production of ROS (i.e. mitochondria) (48). Therefore, our results suggest that a PCD mechanism involving subcellular redistributions in cell death proteins may participate in the pathogenesis of ALS.

The degeneration of motor neurons in individuals with ALS has many similarities to the apoptosis of CNS neurons induced by axotomy and target deprivation in adult animals (10, 22, 25), including sciatic nerve avulsion-induced apoptosis of motor neurons (26). The degeneration of target-deprived neurons that will die is characterized morphologically by chromatolysis followed by a progressive sequence of neurofilament accumulation, cytoplasmic and nuclear condensation, and cellular shrinkage that culminates in apoptosis (10, 22, 25, 26). Degenerating motor neurons in ALS also undergo chromatolysis and then progressive cytoplasmic and nuclear condensation. Affected neurons show cytoskeletal pathology in the form of neurofilament accumulation within the neuronal cell body and axon (49, 50). We assume in our proposed cytopathological staging scheme for motor neuron degeneration in ALS that neurons with different severities of somatodendritic attrition are at different stages of a single, progressive cell death process. Interestingly, the nuclear morphology of degenerating motor neurons in individuals with ALS (Fig. 2) was not identical to classical neuronal apoptosis found in the developing CNS (21, 23, 24) or to excitotoxicity-induced neuronal apoptosis in the developing brain (21, 22). Therefore, we conclude that the death of neurons in ALS is a form of apoptosis that may differ slightly from classical apoptosis at the structural level. This interpretation is consistent with the concept that neuronal maturity, magnitude of target deprivation, and rate (i.e. progression or timing) of neuronal death may influence the structure of dying cells (22, 24, 51).

The structure of motor neuron degeneration in ALS may be a variant of apoptosis because multiple forms of PCD may exist (21, 24, 51). Motor neuron death in ALS could be autophagic (or type 2), according to the classification of Clarke (24), but the presence of autophagy in degenerating motor neurons in ALS is unclear. Some motor neurons in ALS contain cytoplasmic inclusions (52–54), such as Bunina bodies and eosinophilic hyaline inclusions (see Fig. 1C for a hyaline inclusion). Bunina bodies may represent autophagic vacuoles (52), although they may also be related to the endoplasmic reticulum (53) or Golgi apparatus (55). Hylaine inclusions are ubiquitinated (54); thus signifying non-lysosomal degradation of abnormal proteins, but nevertheless supporting a possible role for programmed autophagy in motor neuron death. It is possible that motor neuron death in ALS therefore exists as a combination of classical apoptosis or Clarke's type 1 degeneration and autophagic death or Clarke's type 2 degeneration (24). Alternatively, the neuronal death pathway identified in this study may not be the sole pathway for neuronal cell death in ALS.

The degeneration of motor neurons in sporadic and familial ALS described here appears to be different structurally from the motor neuron degeneration found in transgenic mice overexpressing the FALS mutant forms of SOD1 (2, 3, 56) and in transgenic mice overexpressing normal and mutant neurofilament proteins (57–59). Neither morphological nor biochemical evidence for apoptotic death of motor neurons has been shown in any of the SOD1 or neurofilament transgenic mouse models of ALS, and it is still uncertain whether motor neurons in these models die or whether they remain in a severely vacuolated, atrophic state. Although the survival of FALS mice is prolonged when crossed with mice overexpressing Bcl-2 (60) or a dominant negative inhibitor of caspase-1 (61), the degeneration of motor neurons is not prevented (60), suggesting that neuronal degeneration in FALS mice might not be apoptosis controlled by PCD mechanisms. The vacuolar and edematous degeneration of motor neurons in mice overexpressing mutant SOD1 (2, 3, 56) or neurofilament protein (57–59) more closely resembles excitotoxic neurodegeneration (51, 62) or transsynaptic neuronal atrophy (but not death) in response to deafferentation (63). Interestingly, the degeneration of motor neurons in individuals with ALS is also different structurally from the excitotoxic neurodegeneration in vivo caused by acute activation of NMDA and non-NMDA glutamate receptors in the mature CNS and by cerebral ischemia (22, 51, 62, 63). However, we have found recently in adult animal models of peripheral nerve avulsion that motor neuron degeneration is apoptosis (26). We therefore conclude that the neuronal degeneration in ALS most closely resembles neuronal apoptosis induced by target deprivation in the mature CNS (10, 22, 25, 26), and is thus possibly related to the deficiency in neurotrophic factors that occurs in individuals with ALS (64). Trophic factor deprivation-induced motor neuron apoptosis in vitro (65–67) and in vivo (65, 66) is caspase- and Bax-dependent, as might be the case for motor neuron apoptosis in ALS.

ACKNOWLEDGMENTS

This article is dedicated to the memory of my father-in-law, William J. Golden. The author is grateful for the technical support of Ann C. Price and for the discussions on cell death with Drs. Carlos Portera-Cailliau, Stephen Ginsberg, and Nael Al-Abdulla.

REFERENCES

1. Kuncl RW, Crawford TO, Rothstein JD, Drachman DB. Motor neuron diseases. In: Asbury, AK, McKhann GM, McDonald WI, eds. Diseases of the nervous system. Clinical neurobiology, Philadelphia: WB Saunders, 1992;1179–208
2. Gurney ME, Pu H, Chiu AY, et al. Motor neuron degeneration in mice that express a human Cu,Zn superoxide dismutase mutation. Science 1994:264:1772–75
3. Wong PC, Pardo CA, Borchelt DR, et al. An adverse property of a familial ALS-linked SOD1 mutation causes motor neuron disease characterized by vacuolar degeneration of mitochondria. Neuron 1995;14:1105–16
4. Rosen DR, Siddique T, Patterson D, et al. Mutations in Cu, Zn superoxide dismutase gene are associated with familial amyotrophic lateral sclerosis. Nature 1993;362:59–62
5. Deng H-X, Hentati A, Tainer JA, et al. Amyotrophic lateral sclerosis and structural defects in Cu,Zn superoxide dismutase. Science 1993;261:1047–51
6. Rabizadeh S, Butler Gralla E, Borchelt DR, et al. Mutations associated with amyotrophic lateral sclerosis convert superoxide dismutase from an antiapoptotic gene to a proapoptotic gene: studies in yeast and neural cells. Proc Natl Acad Sci USA 1995;92:3024–28
7. Ghadge GD, Lee JP, Bindokas VP, et al. Mutant superoxide dismutase-1-linked familial amyotrophic lateral sclerosis: Molecular mechanisms of neuronal death and protection. J Neurosci 1997;17: 8756–66
8. Troy CM, Shelanski ML. Down-regulation of copper/zinc superoxide dismutase causes apoptotic death in PC12 neuronal cells. Proc Natl Acad Sci USA 1994;91:6384–87
9. Greenlund LJS, Deckwerth TL, Johnson EM. Superoxide dismutase delays neuronal apoptosis: A role for reactive oxygen species in programmed neuronal death. Neuron 1995;14:303–15
10. Al-Abdulla NA, Martin LJ. Apoptosis of retrogradely degenerating neurons occurs in association with the accumulation of perikaryal mitochondria and oxidative damage to the nucleus. Am J Pathol 1998;153:447–56
11. Hamburger V. Cell death in the development of the lateral motor column of the chick embryo. J Comp Neurol 1975;160:535–46
12. Yan Q, Elliot JL, Matheson C, et al. Influences of neurotrophins on mammalian motoneurons *in vivo*. J Neurobiol 1993;24:1555–77
13. Abe K, Pan L-H, Watanabe M, Kato T, Itoyama Y. Induction of nitrotyrosine-like immunoreactivity in the lower motor neuron of amyotrophic lateral sclerosis. Neurosci Lett 1995;199:152–54
14. Ferrante RJ, Browne SE, Shinobu LA, et al. Evidence of increased oxidative damage in both sporadic and familial amyotrophic lateral sclerosis. J Neurochem 1997;69:2064–74
15. Mu X, He J, Anderson DW, Trojanowski JQ, Springer JE. Altered expression of *bcl-2* and *bax* mRNA in amyotrophic lateral sclerosis spinal cord motor neurons. Ann Neurol 1996;40:379–86
16. Lefebvre S, Bürglen L, Reboullet S, et al. Identification and characterization of a spinal muscular atrophy-determining gene. Cell 1995;80:155–65
17. Roy N, Mahadevan MS, McLean M, et al. The gene for neuronal apoptosis inhibitory protein is partially deleted in individuals with spinal muscular atrophy. Cell 1995;80:167–78
18. Yoshiyama Y, Yamada T, Asanuma K, Asahi, T. Apoptosis related antigen, Le^Y and nick-end labeling are positive in spinal motor neurons in amyotrophic lateral sclerosis. Acta Neuropathol 1994;88: 207–11
19. Migheli A, Cavalla P, Marino S, Schiffer D. A study of apoptosis in normal and pathologic nervous tissue after in situ end-labeling of DNA strand breaks. J Neuropathol Exp Neurol 1994;53:606–16
20. Troost D, Aten J, Morsink F, de Jong JMBV. Apoptosis in amyotrophic lateral sclerosis is not restricted to motor neurons. Bcl-2 expression is increased in unaffected post-central gyrus. Neuropathol Appl Neurobiol 1995;21:498–504
21. Portera-Cailliau C, Price DL, Martin LJ. Excitotoxic neuronal death in the immature brain is an apoptosis-necrosis morphological continuum. J Comp Neurol 1997;378:70–87
22. Martin LJ, Al-Abdulla NA, Brambrink AM, Kirsch JR, Sieber FE, Portera-Cailliau C. Neurodegeneration in excitotoxicity, global cerebral ischemia, and target deprivation: A perspective on the contributions of apoptosis and necrosis. Brain Res Bull 1998;46: 281–309
23. Chu-Wang I-W, Oppenheim RW. 1978. Cell death of motoneurons in the chick embryo spinal cord. I. A light and electron microscopic study of naturally occurring and induced cell loss during development. J Comp Neurol 1978;177:33–58
24. Clarke PGH. Developmental cell death: Morphological diversity and multiple mechanisms. Anat Embryol 1990;181:195–213
25. Al-Abdulla NA, Portera-Cailliau C, Martin LJ. Occipital cortex ablation in adult rat causes retrograde neuronal death in the lateral geniculate nucleus that resembles apoptosis. Neuroscience 1998;86: 191–209
26. Martin LJ, Kaiser A, Price AC. Motor neuron degeneration after sciatic nerve avulsion in adult rat evolves with oxidative stress and is apoptosis. J Neurobiol (in press)
27. Liu X, Zou H, Slaughter C, Wang X. DFF, a heterodimeric protein that functions downstream of caspase-3 to trigger DNA fragmentation during apoptosis. Cell 1997;89:175–84
28. Wiedenmann B, Franke WW. Identification and localization of synaptophysin, an integral membrane glycoprotein of M_r 38,000 characteristic of presynaptic vesicles. Cell 1985;42:1017–28
29. Perry G, Nunomura A, Smith MA. A suicide note from Alzheimer disease neurons? Nat Med 1998;4:897–98
30. Krajewsk S, Krajewska M, Shabaik A, Miyashita T, Wang HG, Reed JC. Immunohistochemical determination of in vivo distribution of bax, a dominant inhibitor of bcl-2. Am J Pathol 1994;145: 1323–36
31. Gross A, Jockel J, Wei MC, Korsmeyer SJ. Enforced dimerization of BAX results in its translocation, mitochondrial dysfunction and apoptosis. EMBO J 1998;17:3878–85
32. Chittenden T, Harrington EA, O'Connor R, et al. Induction of apoptosis by the Bcl-2 homologue Bak. Nature 1995;374:733–36
33. Merry DE, Veis DJ, Hickey WF, Korsmeyer SJ. Bcl-2 protein expression is widespread in the developing nervous system and retained in the adult PNS. Development 1994;120:310–11
34. Lithgow T, van Driel R, Bertram JF, Strasser A. The protein product of the oncogene *bcl-2* is a component of the nuclear envelope, the endoplasmic reticulum, and the outer mitochondrial membrane. Cell Growth Differ 1994;5:411–17
35. Boise LH, González-García M, Postema C, et al. Bcl-x, a bcl-2-related gene that functions as a dominant regulator of apoptotic cell death. Cell 1993;74:597–608
36. González-García M, García I, Ding L, et al. Bcl-x is expressed in embryonic and postnatal neural tissues and functions to prevent neuronal cell death. Proc Natl Acad Sci USA 1995;92:4304–8
37. Merry DE, Korsmeyer SJ. Bcl-2 gene family in the nervous system. Ann Rev Neurosci 1997;20:245–67
38. Hsu Y-T, Youle RJ. Nonionic detergents induce dimerization among members of the Bcl-2 family. J Biol Chem 1997;272:13829–34
39. Antonsson B, Conti F, Ciavatta A, et al. Inhibition of bax channel-forming activity by bcl-2. Science 1997;277:370–72
40. Li P, Nijhawan D, Budihardjo I, et al. Cytochrome c and dATP-dependent formation of Apaf-1/caspase-9 complex initiates an apoptotic protease cascade. Cell 1997;91:479–89
41. Liu X, Kim CN, Yang J, Jemmerson R, Wang, X. Induction of apoptotic program in cell-free extracts: requirement for dATP and cytochrome c. Cell 1996;86:147–57

42. Kluck RM, Bossy-Wetzel E, Green DR, Newmeyer DD. The release of cytochrome c from mitochondria: A primary site for bcl-2 regulation of apoptosis. Science 1997;275:1132–36
43. Yang J, Liu X, Bhalla K, et al. Prevention of apoptosis by bcl-2: release of cytochrome c from mitochondria blocked. Science 1997;275:1129–32
44. Liu X, Li P, Widlak P, et al. The 40-kDa subunit of DNA fragmentation factor induces DNA fragmentation and chromatin condensation during apoptosis. Proc Natl Acad Sci USA 1998;95:8461–66
45. Vander Heiden MG, Chandel NS, Williamson EK, Schumaker PT, Thompson CB. Bcl-x_L regulates the membrane potential and volume homeostasis of mitochondria. Cell 1997;91:627–37
46. Wolter KG, Hsu Y-T, Smith CL, Nechushtan A, Xi X-G, Youle RJ. Movement of Bax from the cytosol to mitochondria during apoptosis. J Cell Biol 1997;139:1281–92
47. Hsu Y-T, Wolter KG, Youle RJ. Cytosol-to-membrane redistribution of Bax and Bcl-x_L during apoptosis. Proc. Natl. Acad. Sci. USA 1997;94:3668–72
48. Hockenbery DM, Oltvai ZN, Yin X-M, Milliman CL, Korsmeyer SJ.Bcl-2 functions in an antioxidant pathway to prevent apoptosis. Cell 1993;75:241–51
49. Kato T, Hirano A, Kurland LT. Asymmetric involvement of the spinal cord involving both large and small anterior horn cells in a case of familial amyotrophic lateral sclerosis. Clin Neuropathol 1987;6:67–70
50. Munoz DG, Greene C, Perl DP, Selkoe DJ. Accumulation of phosphorylated neurofilaments in anterior horn motoneurons of amyotrophic lateral sclerosis patients. J Neuropathol Exp Neurol 1988;47:9–18
51. Portera-Cailliau C, Price DL, Martin LJ. Non-NMDA and NMDA receptor-mediated excitotoxic neuronal deaths in adult brain are morphologically distinct: further evidence for an apoptosis-necrosis continuum. J Comp Neurol 1997;378:88–104
52. Hart MN, Cancilla PA, Frommes S, Hirano A. Anterior horn cell degeneration and Bunina-type inclusions associated with dementia. Acta Neuropathol 1977;38:225–28
53. Tomonaga M, Saito M, Yoshimura H, Shimada H, Tohgi H. Ultrastructure of the Bunina bodies in anterior horn cells of amyotrophic lateral sclerosis. Acta Neuropathol 1978;42:81–86
54. Kato T, Katagiri T, Hirano A, Kawanami T, Sasaki H. Lewy body-like hyaline inclusions in sporadic motor neuron disease are ubiquitinated. Acta Neuropathol 1989;77:391–96
55. Okamoto K, Hirai S, Amari M, Watanabe M, Sakurai A. Bunina bodies in amyotrophic lateral sclerosis immunostained with rabbit anti-cystatin C serum. Neurosci Lett 1993;162:125–28
56. Dal Canto MC, Gurney ME. Development of central nervous system pathology in a murine transgenic model of human amyotrophic lateral sclerosis. Am J Pathol 1994;145:1271–80
57. Xu Z, Cork LC, Griffin JW, Cleveland DW. Increased expression of neurofilament subunit NF-L produces morphological alterations that resemble the pathology of human motor neurons disease. Cell 1993;73:23–33
58. Côté F, Collard J-F, Julien J-P. Progressive neuronopathy in transgenic mice expressing the human neurofilament heavy gene: A mouse model of amyotrophic lateral sclerosis. Cell 1993;73:35–46
59. Lee MK, Marszalek JR, Cleveland DW. A mutant neurofilament subunit causes massive, selective motor neuron death: implications for the pathogenesis of human motor neuron disease. Neuron 1994;13:975–88
60. Kostic V, Jackson-Lewis V, de Bilbao F, Dubois-Dauphin M, Przedborski S. Bcl-2: Prolonging life in a transgenic mouse model of familial amyotrophic lateral sclerosis. Science 1997;277:559–62
61. Friedlander RM, Brown RH, Gagliardini V, Wang J, Juan J. Inhibition of ICE slows ALS in mice. Nature 1997;388:31
62. Ikonomidou C, Qin YQ, Labruyere J, Olney JW. Motor neuron degeneration induced by excitotoxin agonists has features in common with those seen in the SOD-1 transgenic mouse model of amyotrophic lateral sclerosis. J Neuropathol Exp Neurol 1996;55:211–24
63. Ginsberg SD, Portera-Cailliau C, Martin LJ. Fimbria-fornix transection and excitotoxicity produce similar neurodegeneration in the septum. Neuroscience 1999;88:1059–71
64. Anand P, Parrett A, Martin J, et al. Regional changes of ciliary neurotrophic factor and nerve growth factor levels in post mortem spinal cord and cerebral cortex from patients with motor disease. Nature Med 1995;1:168–72
65. Milligan CE, Prevette D, Yaginuma H, et al. Peptide inhibitors of the ICE protease family arrest programmed cell death of motoneurons in vivo and in vitro. Neuron 1995;15:385–93
66. Deckwerth TL, Elliott JL, Knudson CM, Johnson EM, Snider WD, Korsmeyer SJ. Bax is required for neuronal death after trophic factor deprivation and during development. Neuron 1996;17:401–11
67. Estévez AG, Spear N, Manuel SM, et al. Nitric oxide and superoxide contribute to motor neuron apoptosis induced by trophic factor deprivation. J Neurosci 1998;18:923–31

Received November 23, 1998
Revision received February 2, 1999
Accepted February 3, 1999